

Tumor-suppressive *microRNA-223* targets *WDR62* directly in bladder cancer

SATOSHI SUGITA, HIROFUMI YOSHINO, MASAYA YONEMORI, KAZUTAKA MIYAMOTO,
RYOSUKE MATSUSHITA, TAKASHI SAKAGUCHI, TOSHIHIKO ITESAKO, SHUICHI TATARANO,
MASAYUKI NAKAGAWA and HIDEKI ENOKIDA

Department of Urology, Graduate School of Medical and Dental Sciences, Kagoshima University, Kagoshima 890-8520, Japan

Received August 7, 2018; Accepted March 14, 2019

DOI: 10.3892/ijo.2019.4762

Abstract. *miRNA-223* (*miR-223*) has been reported to function not only as a tumor suppressor, but also as an oncogenic microRNA (*miRNA* or *miR*) in various cancer cells. Therefore, the functional role of *miR-223* has not been elucidated to date, at least to the best of our knowledge. We previously performed the deep sequencing analysis of clinical bladder cancer (BC) specimens. It was revealed that *miR-223* expression was significantly downregulated in BC, suggesting that *miR-223* functions as a tumor suppressor *miRNA* in BC. The aim of this study was to investigate the functional roles of *miR-223* and to identify its targets in BC. The expression levels of *miR-223* were significantly decreased in our clinical BC specimens. The Cancer Genome Atlas (TCGA) database indicated that *miR-223* expression was related to lymphovascular invasion and distant metastasis. The restoration of *miR-223* expression significantly inhibited tumor aggressiveness and induced apoptosis via caspase-3/7 activation in BC cells. *WD repeat domain 62* (*WDR62*), a candidate target of *miR-223* according to *in silico* analyses, has been previously proposed to play a role in neurodevelopment. Direct binding between *WDR62* and *miR-223* was confirmed by luciferase assay. The TCGA database revealed positive associations between *WDR62* mRNA expression and a higher tumor grade and stage in BC. The knockdown of *WDR62* significantly inhibited tumor aggressiveness and induced the apoptosis of BC cells. On the whole, the findings of this study reveal a novel *miR-223* target, oncogenic *WDR62*, and provided insight into the oncogenesis of BC.

Introduction

Bladder cancer (BC) was the fifth most common type of cancer and the eighth most common cause of cancer-related mortality among 40 countries investigated in 2012 (1). In fact, 429,800 new cases of BC were diagnosed, and 165,000 patients succumbed to the disease worldwide in 2012 (2). The 5-year survival rate of patients with BC has improved by only a small percentage over the past 30 years according to Surveillance, Epidemiology and End Results (SEER) program of the National Cancer Institute. Patients with metastasis are generally treated with cisplatin-based combination chemotherapy, although its efficacy is limited (3). Standard chemotherapy as a first-line therapy has shifted from the methotrexate, vinblastine, doxorubicin and cisplatin (MVAC) regimen to the gemcitabine and cisplatin (GC) regimen over the past several years due to the lower toxicity of GC. However, GC therapy has not conferred an overall survival benefit to patients with BC compared with MVAC therapy (4). Therefore, the 5-year survival rate of patients with lymph node or distant metastasis remains <20% (5). A main reason behind the fact that the 5-year survival rate of patients with BC has not markedly improved is that the mechanisms of recurrence and metastasis in BC have not yet been sufficiently elucidated.

MicroRNAs (*miRNAs* or *miRs*) are endogenous small non-coding RNAs (19-22 nucleotides in length) that negatively regulate protein-coding genes by binding to the 3'-untranslated region (UTR) of the target mRNA and inhibiting transcriptional or post-transcriptional expression (6). A single *miRNA* is able to regulate thousands of target transcripts, and >60% of protein-coding genes may be regulated by *miRNAs* (7,8). It has previously been demonstrated that *miRNAs* are aberrantly expressed in various human malignancies and play significant roles in oncogenesis and metastasis (9). Therefore, the detection of aberrantly expressed *miRNAs* and their target genes is an important step for elucidating *miRNA*-regulated oncogenic pathways.

Our previous study on BC *miRNA* profiles revealed significantly downregulated *miRNAs* in BC tissues compared with normal bladder tissues (10). According to the profile, we have previously demonstrated that several *miRNAs* function as tumor suppressors by targeting numerous oncogenes in BC cells (11-16). In the current study, we focused on *miRNA-223* (*miR-223*), which

Correspondence to: Dr Hideki Enokida, Department of Urology, Graduate School of Medical and Dental Sciences, Kagoshima University, 8-35-1 Sakuragaoka, Kagoshima 890-8520, Japan
E-mail: enokida@m.kufm.kagoshima-u.ac.jp

Key words: bladder cancer, microRNA, *miR-223*, tumor suppressor, *WD repeat domain 62*

was also listed as one of the top 50 downregulated miRNAs in the profile. *miR-223* has been reported to function not only as a tumor suppressor, but also as an oncogenic miRNA in different types of cancer cells. In BC, only two reports to date have demonstrated the tumor-suppressive functions of *miR-223* (17,18), at least to the best of our knowledge. However, the functional roles of *miR-223* have not been sufficiently elucidated in BC. Thus, the aim of this study was to investigate further the functional significance of *miR-223* and to identify the novel molecular targets of this miRNA in BC. The identification of novel molecular targets of *miR-223* could provide important information on BC oncogenesis and may thus lead to the development of novel therapeutic strategies for BC.

Material and methods

Clinical specimens and cell culture. Clinical specimens were collected from patients with BC (n=32) who had undergone cystectomy (n=6) or transurethral resection of their bladder tumors (n=26) at the Kagoshima University Hospital (Kagoshima, Japan) from 2004 to 2013. Normal bladder epithelial (NBE; n=12) specimens were derived from patients with non-cancerous diseases. The specimens were staged according to the American Joint Committee on Cancer (AJCC)/Union Internationale Contre le Cancer (UICC) tumor-node-metastasis classification system and were histologically graded. This study was approved by the Bioethics Committee of Kagoshima University; the study numbers were H27-104 and H27-105. Written informed consent and approval were obtained from all patients prior to obtaining the samples. The clinicopathological characteristics of the patients are presented in Table I.

In addition, we used two human BC cell lines: Invasive T24 cells, which were obtained from the American Type Culture Collection (ATCC, Manassas, VA, USA: cat. no. HTB-4) and BOY cells, which were established in our laboratory from an Asian male patient, 66 years of age, given a diagnosis of stage III BC with lung metastasis. These cell lines were maintained in the recommended media containing 10% fetal bovine serum (FBS) in a humidified atmosphere of 95% air at 37°C. Eagle's minimum essential medium (MEM) was used for the culture medium for the BOY cells. These cell lines were subjected to the experiments at passage numbers between 10 and 20. Regularly, mycoplasma testing was carried out for the cell lines and no infection was confirmed. We found no information regarding misidentified or cross-contaminated cell lines; the all cell lines used were cross-checked from the International Cell Line Authentication Committee (<http://iclac.org/databases/cross-contaminations/>) and ExPASy Cellosaurus databases (<https://web.expasy.org/cellosaurus/>).

Tissue collection and RNA extraction. Tissues were treated with RNAlater (Thermo Fisher Scientific, Waltham, MA, USA) and stored at -20°C until RNA extraction. Total RNA, including miRNAs, was extracted from the tissues and the cells using the mirVana miRNA Isolation kit (Thermo Fisher Scientific) and Isogen (Nippon Gene, Tokyo, Japan), respectively following the manufacturer's protocol.

Reverse transcription-quantitative PCR (RT-qPCR). Stem-loop RT-PCR (TaqMan MicroRNA Assay for *miR-223*; P/N 002295;

Applied Biosystems, Foster City, CA, USA) was used for RT-qPCR to evaluate miRNA expression levels according to previously published methods (11). We used human *RNU48* (P/N 001006; Applied Biosystems) as an internal control and employed the $\Delta\Delta C_q$ method to calculate the fold changes in expression (12). For *WDR62* and *glucuronidase beta* (*GUSB*) expression, we applied a SYBR-Green qPCR system using the following primers: *WDR62* forward, 5'-GCCTTCTCACCCAA TATGAAGC-3' and reverse, 5'-GCCTTCTCACCCAATATGA AGC-3'; and *GUSB* forward, 5'-CGTCCCACCTAGAATCT GCT-3' and reverse, 5'-TTGCTCACAAAGGTCACAGG-3'. We also performed RT-qPCR analyses of the 11 genes that were significantly upregulated in the TCGA cohort of BC. The primers for detecting expressions of those genes are described in Table III. For the reverse transcription step, 500 ng total RNA was reverse transcribed into cDNA using the High Capacity cDNA Reverse Transcription kit (Thermo Fisher Scientific, Inc.) under the incubation conditions of 25°C for 10 min, 37°C for 120 min and 85°C for 5 min. qPCR was performed using a Power SYBR-Green Master Mix (cat. no. 4367659) on a 7300 Real-time PCR System (both Applied Biosystems; Thermo Fisher Scientific, Inc.). Furthermore, the initial step time for activation was 10 min at 95°C, followed by 40 cycles between a denaturation step for 15 sec at 95°C and an annealing/extension step for 1 min at 60°C.

The specificity of amplification was monitored according to the dissociation curve of the amplified product. All expression values were normalized to those for *GUSB*, and the $\Delta\Delta C_q$ method was employed to calculate the fold change values (12). All experiments were performed in triplicate.

Transfection of miRNAs, siRNAs and anti-miRNAs. As previously described (11), the T24 and BOY cells were transfected with 10 nM mature miRNA, siRNA or anti-miRNA using Lipofectamine RNAiMAX transfection reagent and Opti-MEM (both from Thermo Fisher Scientific). Mature miRNA molecules, Pre-miR™ miRNA precursors (*miR-223*, *hsa-miR-223-3p*, P/N PM12301; Thermo Fisher Scientific) and negative control miRNA (P/N AM17111; Thermo Fisher Scientific) were used for the gain-of-function experiments, whereas two different *WDR62* siRNA (P/N HSS138565 and HSS138567; Thermo Fisher Scientific), negative control siRNA (P/N D-001810-10; Thermo Fisher Scientific), *mirVana*® miRNA inhibitor (*anti-miR-223*, *hsa-miR-223-3p*, P/N MH12301; Thermo Fisher Scientific) and negative control miRNA inhibitor (P/N AM17010; Thermo Fisher Scientific) were used for the loss-of-function experiments. For co-transfection, the BC cells were simultaneously transfected with 10 nM *miR-223* and 10 nM *anti-miR-223* using Lipofectamine RNAiMAX and Opti-MEM (both from Thermo Fisher Scientific).

Cell viability, migration and invasion assays. In order to investigate the functional significance of *miR-223* and *WDR62*, we performed cell viability, migration and invasion assays using the T24 and BOY cells transfected with 10 nM miRNA or siRNA by reverse transfection. The cells were seeded in 96-well plates at 3×10^3 /well for XTT assays. After 72 h, cell viability was determined using the Cell Proliferation kit II (Roche Diagnostics GmbH, Mannheim, Germany) as previously described (11). The cell migration ability was

evaluated using wound healing assays. Cells were plated in 6-well plates at 2×10^5 /well, and after 48 h of transfection, the cell monolayer was scratched using a P-20 micropipette tip. The initial gap length (0 h) and residual gap length at 24 h after wounding were calculated from photomicrographs by using an OLYMPUS CK2 microscope (Olympus Optical Corp., Tokyo Japan) as previously described (13). Cell invasion assays were assessed by modified Boyden chambers consisting of Transwell pre-coated Matrigel membrane filter inserts with 8-micrometer pores in 24-well tissue culture plates (BD Biosciences, Bedford, MA, USA). At 72 h following transfection, the cells were seeded in the upper chamber of 24-well plates at 1×10^5 /well with serum-free Eagle's MEM. After 24 h, 37°C incubation. MEM containing 10% FBS in the lower chamber served as the chemoattractant, as previously described (11). The cells were stained by Diff-Quick (a modified Giemsa stain) (Richard Allan Scientific, San Diego, CA, USA). Briefly, the cells were fixed with pure methanol for 2 min, followed by stained by the dye I and dye II each for 2 min. The number of the cells on the surface of the chamber was counted by using OLYMPUS BX41 (Olympus Optical Corp.). All experiments were performed in triplicate.

Colony formation assay. For colony formation assays to examine effects of WDR62 knockdown, the cells transfected with 10 nM siRNA were seeded into 10-cm dish at a density of 1,000 cells/well. Following 7 days of incubation in the MEM containing 10% FBS in a humidified atmosphere of 95% air at 37°C, the resulting colonies were fixed with 4% paraformaldehyde phosphate buffer solution (Nacalai Tesque, Kyoto, Japan) and stained with 0.04% crystal violet (Nacalai Tesque) for 10 min at room temperature. The numbers of colonies were counted. The average colony density was calculated and expressed as the relative percentage of the mock group (only with opti-MEM Lipofectamine RNAiMAX).

Apoptosis assays. The BC cell lines were transfected with reagent only (mock), miR-control, miR-223, siRNA-control or si-WDR62 at the concentration of 10 nM in 6-well tissue culture plates, as described previously (14). The cells were harvested by trypsinization at 72 h following transfection and washed in cold phosphate-buffered saline. For the apoptosis assays, double staining with FITC-Annexin V and propidium iodide was performed using the FITC Annexin V Apoptosis Detection kit (BD Biosciences) according to the manufacturer's recommendations and analyzed within 1 h by flow cytometry (CytoFLEX analyzer; Beckman Coulter, Brea, CA, USA). Cells were identified as viable, dead, early apoptotic or apoptotic cells using CytExpert™ 1.2 software (Beckman Coulter), and the percentages of early apoptotic and apoptotic cells in each experiment were then compared.

Caspase-3/7 activity assays. Caspase-3/7 activity was measured using CellEvent™ caspase-3/7 Green Detection Reagent (Invitrogen/Thermo Fisher Scientific). BC cell lines in a 96-well plate were transfected with mature miRNAs and siRNAs as described above. After 72 h, 5 μM CellEvent™ caspase-3/7 Green Detection Reagent were added to each well and incubated at 37°C for 30 min. The fluorescence was then measured in each well. For densitometric analysis, the

total fluorescence was quantitated using the BZ-II Analyzer (Keyence, Osaka, Japan). Experiments were performed in triplicate.

Cell cycle assays. For cell cycle analyses, the cells were fixed in 70% aqueous ethanol and stained with propidium iodide at 4°C for 30 min following treatment with RNase A as previously described (15). The data were analyzed using the CytoFLEX analyzer (Beckman Coulter). The percentages of cells in the G0/G1, S and G2/M phases were determined and compared. Experiments were performed in triplicate. We used 1 μg/ml nocodazole (P/N ab120630; Abcam, Cambridge, UK) to induce G2/M arrest in each cell line as previously described (16). Experiments were done in triplicate.

Western blot analysis. Following 3 days of transfection, total protein lysate was prepared with a radioimmunoprecipitation assay (RIPA) buffer (Thermo Fisher Scientific, Inc.) containing protease inhibitor cocktail (Sigma-Aldrich; Merck KGaA). The protein concentrations were determined using the Bradford assay (17). Protein lysate (20 μg) per lane was loaded in NuPAGE on 4-12% bis-tris gel (Invitrogen/Thermo Fisher Scientific) and transferred into a polyvinylidene fluoride membrane. Following transfer, the membranes were blocked in washing buffer (0.35 M NaCl, 10 mM Tris-HCl, pH 8.0, and 0.05% Tween-20) containing 3% skim milk for 2 h at room temperature, followed by an overnight incubation at 4°C with rabbit anti-WDR62 antibodies (1:500, P/N GTX119724; GeneTex, San Antonio, TX, USA), anti-cleaved poly (ADP-ribose) polymerase (PARP) antibodies (1:1,000, P/N 5625), anti-cleaved caspase-3 antibodies (1:1,000, P/N 9664) (both from Cell Signaling Technology, Danvers, MA, USA) and anti-β-actin antibodies (1:1,000, P/N bs-0061R; Bioss, Woburn, MA, USA). The secondary antibodies were peroxidase-labelled anti-rabbit IgG (1 h at 25°C; 1:5,000; cat. no. 7074S; Cell Signaling Technology, Inc.). Specific complexes were visualized using an echochemiluminescence detection system (GE Healthcare, Little Chalfont, UK) as previously described (13).

Immunohistochemistry (IHC). A tissue microarray containing 78 urothelial cancers and 20 normal bladder tissues was obtained from US Biomax, Inc. (product ID: BL 1002; Rockville, MD, USA). Detailed information on all tumor specimens can be found at <http://www.biomax.us/index.php>. The tissue microarray was immunostained following the manufacturer's protocol with an Ultra Vision Detection System (Thermo Fisher Scientific). Primary rabbit polyclonal antibodies against WDR62 (P/N GTX119724; GeneTex) were diluted 1:1,000. Immunostaining was evaluated according to the scoring method described previously (13). Each case was scored on the basis of the intensity and area of staining. The intensity of staining was graded on the following scale: 0, no staining; 1+, mild staining; 2+, moderate staining; and 3+, intense staining. The area of staining was evaluated as follows: 0, no staining of cells in any microscopic field; 1+, <30% of cells stained positive; 2+, 30-60% stained positive; 3+, >60% stained positive. The immunostaining scores (intensity + extent) were combined and analyzed. All samples were independently scored by two of the authors (T.S. and K.M.), who were blinded to the patient status.

In silico analysis to identify the genes regulated by *miR-223*. *In silico* analysis was performed to identify target genes of *miR-223* using the TargetScan database Release 7.1 (http://www.targetscan.org/vert_71/). Additionally, the Gene Expression Omnibus (accession nos. GSE11783 and GSE31684) and The Cancer Genome Atlas (TCGA) databases were used to identify upregulated genes in BC specimens. We merged these datasets and selected possible *miR-223* target genes.

Plasmid construction and dual-luciferase reporter assays. Partial sequences of the wild-type *WDR62* 3'-UTR or the *WDR62* 3'-UTR with deletion of the *miR-223* target site (position 62-69 of the *WDR62* 3'-UTR) and the *miR-223* target site sequence (position 62-69 of the *WDR62* 3'-UTR) were inserted between the *Xho*I and *Pme*I restriction sites within the 3'-UTR of the *hRluc* gene in the psiCHECK-2 vector (P/N C8021; Promega, Madison, WI, USA). The T24 and BOY cells were transfected with 50 ng vector and 10 nM *miR-223* using Lipofectamine 2000 (Thermo Fisher Scientific) and Opti-MEM (Thermo Fisher Scientific). The activities of Firefly and *Renilla* luciferases in the cell lysates were determined using a dual luciferase assay system according to the manufacturer's protocol (P/N E1960; Promega). Normalized data were presented as *Renilla*/Firefly luciferase activity ratios. Experiments were performed in triplicate.

Analysis of TCGA BC datasets. BC samples (n=407) and normal bladder samples (n=19) from the TCGA database were used to analyze the *WDR62* mRNA expression levels in BC compared with normal and BC tissues. BC samples from the TCGA database were used to determine the associations between the expression of *miR-223* or *WDR62* and clinicopathological factors. Gene and miRNA quantification were performed using RNA-seq expression data (normalized RSEM) and miRNA-seq data (reads per million mapped reads) (18). Whole-exome sequencing data were available for the 407 BC samples and 19 normal samples. Full sequencing information and clinical information were acquired using the cBio Portal (<http://www.cbioportal.org/public-portal/>) and TCGA (<https://tcga-data.nci.nih.gov/>).

Statistical analysis. The differences between 2 groups were analyzed using Mann-Whitney U tests. The differences between 3 variables and numerical values were analyzed using Bonferroni-adjusted Mann-Whitney U tests. The overall survival of patients with BC from the TCGA cohort was evaluated by the Kaplan-Meier method. Patients were divided into 2 groups according to the median *miR-223* or *WDR62* expression level, and differences between the 2 groups were evaluated by log-rank tests. All analyses were performed using Expert StatView software, version 5.0 (SAS Institute Inc., Cary, NC, USA). All data are expressed as the means \pm standard deviation. P-values <0.05 were considered to indicate statistically significant differences.

Results

Expression levels of miR-223 in clinical BC specimens and cell lines. First, we evaluated the expression levels of *miR-223* in BC samples (n=32) and NBE samples (n=12) in our facility by

Table I. Patient characteristics.

Bladder cancer (BC)	No.	Range/percentage
Total	32	
Median age (range), years	71.5	(43-93)
Sex		
Male	22	68.8%
Female	10	31.2%
Tumor grade		
Low grade	14	43.7%
High grade	16	50.0%
Unknown	2	6.3%
T stage		
Tis	1	3.1%
Ta	5	15.1%
T1	7	21.9%
T2	11	34.4%
T3	3	9.4%
T4	2	6.3%
Unknown	3	9.4%
N stage		
N0	22	68.8%
N1	3	9.4%
Unknown	7	21.9%
M stage		
M0	28	87.5%
M1	2	6.3%
Unknown	2	6.3%
Surgical method		
TURBT	26	81.3%
Cystectomy	6	18.8%
Normal bladder epithelium		
Total number	12	
Median age (range), years	63.5	(51-75)

TURBT, transurethral resection of bladder tumor.

RT-qPCR. Patient details and clinicopathological characteristics are summarized in Table I. The expression level of *miR-223* was significantly lower in the BC tissues than in the NBE tissues (P=0.013; Fig. 1A). *miR-223* expression was also decreased in the T24 and BOY BC cell lines compared with the NBE samples.

Associations between miR-223 expression and clinicopathological parameters in the TCGA datasets. We evaluated the association between *miR-223* expression and the patient clinicopathological parameters or overall survival. Among the BC cohort of TCGA, we evaluated 407 patients with available *miR-223* expression, clinicopathological and survival data. Among these, data of lymphovascular invasion and distant metastasis were available for 278 and 202 patients, respectively. The expression level of this miRNA was

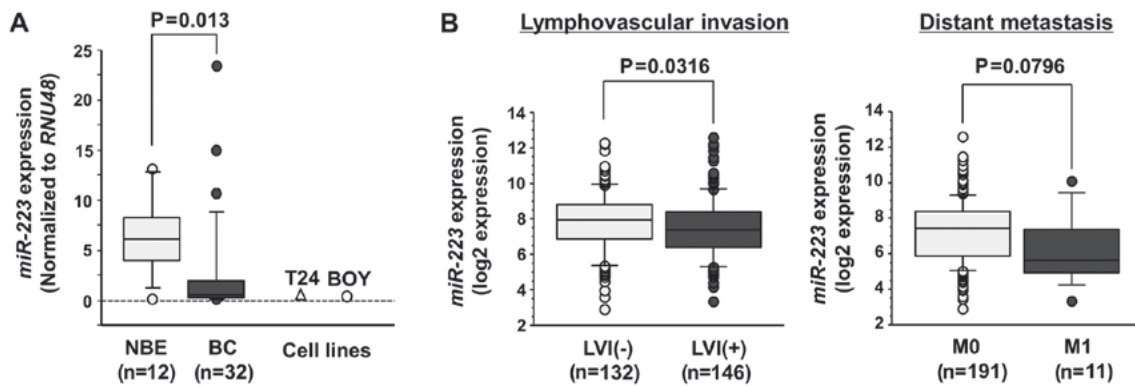


Figure 1. Associations of the expression level of *miR-223* with the patient clinicopathological parameters. (A) The expression level of *miR-223*, determined by RT-qPCR, was significantly lower in the 32 clinical BC specimens than in the 12 adjacent NBE specimens from our facility. (B) The associations between *miR-223* expression and the patient clinicopathological parameters in the BC cohort from the TCGA database were determined using the Mann-Whitney U test. NBE, normal bladder epithelium; BC, bladder cancer.

significantly lower in patients with BC with lymphovascular invasion (LVI) ($P=0.0316$; Fig. 1B, left panel) and had a tendency to be lower in patients with BC with distant metastasis compared with their counterparts ($P=0.0796$; Fig. 1B, right panel). Next, the cohort was divided into 2 groups according to the median *miR-223* expression level. Kaplan-Meier analysis revealed no differences in the overall survival rate between patients with a high ($n=203$) and patients with a low *miR-223* expression ($n=203$) ($P=0.2866$) (data not shown).

Effects of *miR-223* restoration on the viability, migration and invasion of BC cell lines. To investigate the functional roles of *miR-223*, we performed gain-of-function analyses using *miRNA*-transfected T24 and BOY BC cell lines. XTT assays revealed a significant inhibition of the viability of the T24 and BOY cells transfected with *miR-223* in comparison with the mock or *miR*-control transfectants (each $P<0.0001$; Fig. 2A). Wound healing assays demonstrated that the migration activity was significantly suppressed in the *miR-223* transfectants compared with the mock or *miR*-control transfectants (each $P<0.0001$; Fig. 2B). Matrigel invasion assays also demonstrated that the number of invading cells was significantly decreased in the *miR-223* transfectants compared with the mock or *miR*-control transfectants (T24 cells: $P=0.0002$, BOY cells: $P<0.0001$; Fig. 2C).

Effects of *miR-223* restoration on the apoptosis of BC cell lines. As it has been previously reported that *miR-223* promotes the apoptosis of acute myeloid leukemia cell lines (22), in this study, we performed flow cytometric analyses to determine the number of apoptotic cells following the restoration of this *miRNA* into BC cell lines. The numbers of apoptotic cells (apoptotic and early apoptotic cells) were significantly higher in the *miR-223* transfectants than in the mock or *miR*-control transfectants (each $P<0.0001$; Fig. 2D). Moreover, in a caspase-3/7 activity assay, the fluorescence intensity was significantly increased in the *miR-223* transfectants compared with the mock or *miR*-control transfectants (T24 cells: $P=0.0013$, BOY cells: $P=0.0002$; Fig. 2E).

Identification of possible target genes regulated by *miR-223* in BC. To identify the target genes of *miR-223*, we performed

in silico analysis. Fig. 3 shows our strategy used to narrow down possible target genes of *miR-223*. Candidate targets of *miR-223* with one or more conserved *miR-223* binding sites (489 genes) were identified using the TargetScan database, release 7.1 (<http://www.targetscan.org>). Among these candidate genes, 24 genes were upregulated in the GEO database (accession nos. GSE11783 and GSE31684). Moreover, the TCGA database was used to identify genes with a higher expression in the BC samples than in the normal bladder samples. The analysis of the TCGA database revealed that the mRNA expression levels of 11 genes were significantly upregulated in BC. Subsequently, we performed RT-qPCR analyses of these 11 genes to confirm which genes have a lower mRNA expression in the *miR-223* transfectants compared with the mock transfectants (Table II). Table II shows that the 11 genes were candidates which could possibly be targets of *miR-223* in clinical BC. Finally, we focused on *WDR62* as, to date, to the best of our knowledge, there have been no reports on this gene as a target of *miR-223*, while the direct regulation of *integrin alpha 3 (ITGA3)* by *miR-223* has been previously reported in prostate cancer (23).

***WDR62* is a direct target of *miR-223* in BC cells.** We performed RT-qPCR and western blot analyses to investigate whether the restoration of *miR-223* expression downregulates *WDR62* expression in BC cells. The *WDR62* mRNA levels were significantly decreased in the *miR-223* transfectants compared with the mock or *miR*-control transfectants (T24 cells: $P=0.0002$, BOY cells: $P=0.0012$; Fig. 4A). The *WDR62* protein levels were also decreased in the *miR-223* transfectants compared with the mock or *miR*-control transfectants (Fig. 4B). In addition, we performed dual-luciferase reporter assays in the BC cells to determine whether *WDR62* was regulated by *miR-223* directly. As the TargetScan database predicts a binding site for *miR-223* in the 3'-UTR of *WDR62* mRNA (position 62-69), we constructed vectors encoding a partial wild-type *WDR62* mRNA sequence including the *miR-223* binding site in the 3'-UTR. We found a significantly reduced luminescence intensity following the co-transfection of *miR-223* and the vector carrying the wild-type sequences at position 62-69 of the *WDR62* 3'-UTR (each $P<0.0001$), whereas no reduction in luminescence was observed following transfection with a vector in which the binding site had been

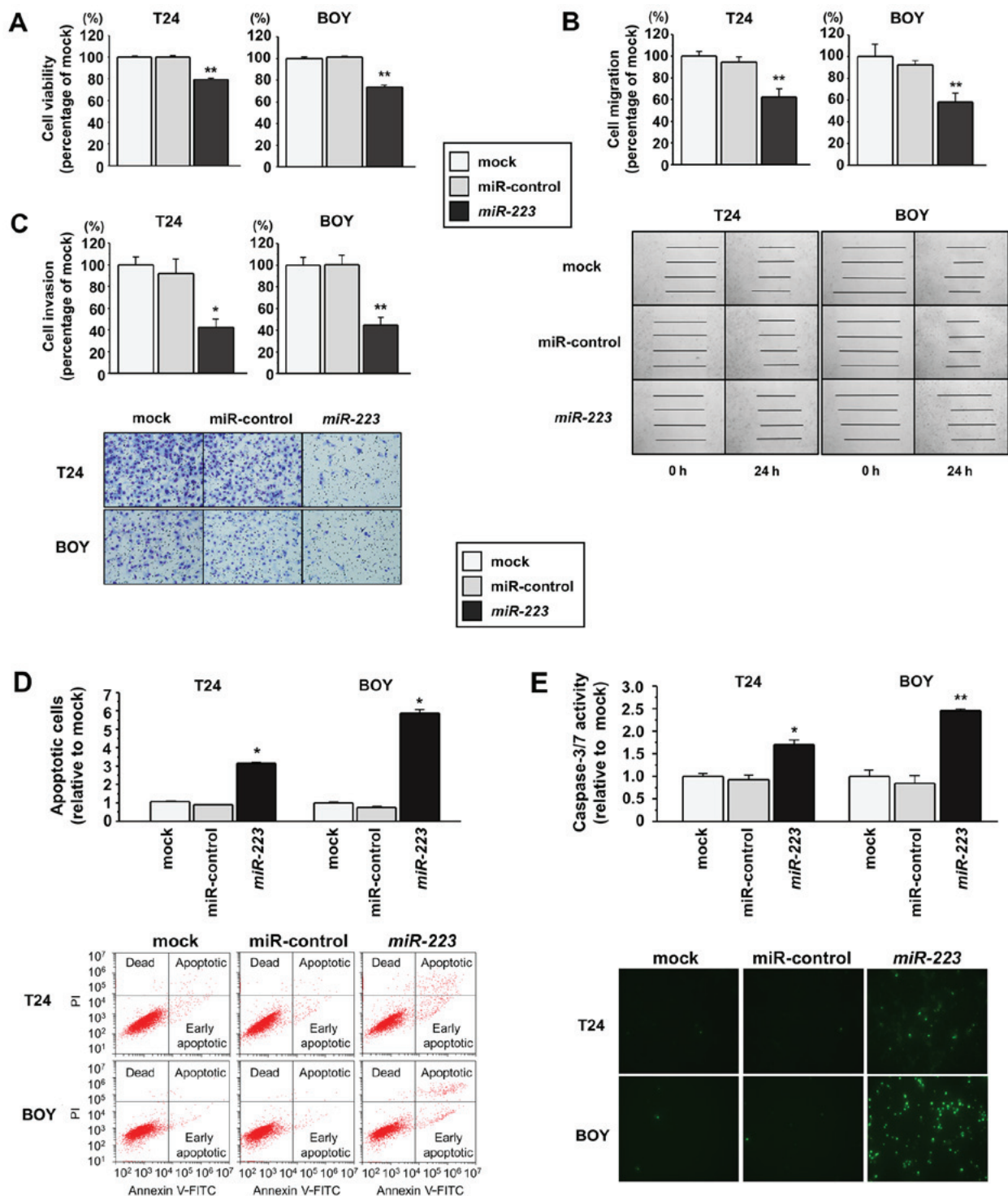


Figure 2. Effects of *miR-223* restoration on BC cell lines. (A-C) Cell viability, migration and invasion were determined by (A) XTT, (B) wound healing and (C) Matrigel invasion assays, respectively. * $P=0.0002$ and ** $P<0.0001$. (D) The numbers of apoptotic cells were evaluated by flow cytometry. The normalized apoptotic cell ratios are presented in the histograms. * $P<0.0001$. (E) Caspase-3/7 activity was measured by a fluorescence based assay. Normalized fluorescence intensity ratios are presented in the histograms. * $P=0.0013$ and ** $P=0.0002$. BC, bladder cancer.

deleted (Fig. 4C). These data suggest that *miR-223* binds directly to the specific site of the 3'-UTR of *WDR62* mRNA.

Associations between WDR62 expression and patient clinicopathological parameters in the TCGA datasets. In a cohort of BC samples ($n=407$) and normal bladder samples ($n=19$) from the TCGA database, the mRNA expression level of *WDR62* was significantly higher in the BC samples than in

the normal bladder samples ($P<0.0001$; Fig. 5A). In addition, we evaluated the associations between *WDR62* expression and the patient clinicopathological parameters or overall survival. Among the BC cohort of TCGA, we evaluated 403 patients with available *WDR62* expression, clinicopathological and survival data. Among these, data of pathological subtype, tumor grade, distant metastasis and clinical were available for 396, 399, 203 and 400 patients, respectively. The mRNA

Table II. Possible candidates of target genes by *in silico* analyses.

Entrez gene ID	Gene symbol	Description	TargetScan omnibus (GEO)			Gene expression		The Cancer Genome Atlas (TCGA)		Knock down efficiency in <i>miR-223</i> transfectants		
			Genomic location	Conserved sites	Poorly conserved sites	Expression	Fold change	Expression	P-value	T24 cells	BOY cells	Average
1	3675	<i>ITGA3</i>	Integrin alpha 3	1	0	Up	3.042	Up	0.0058	0.510	0.122	0.316
2	284403	<i>WDR62</i>	WD repeat domain 62	1	0	Up	3.294	Up	<0.0001	0.599	0.505	0.552
3	1894	<i>ECT2</i>	Ect2 oncogene	1	1	Up	11.070	Up	<0.0001	0.712	0.860	0.786
4	374407	<i>DNAI13</i>	DnaJ (Hsp40) related, subfamily B, member 13	1	0	Up	5.137	Up	0.002	1.377	0.204	0.790
5	1033	<i>CDKN3</i>	Cyclin-dependent kinase inhibitor 3	2	0	Up	10.685	Up	<0.0001	0.655	1.210	0.932
6	10675	<i>CSPG5</i>	Chondroitin sulfate proteoglycan 5	1	0	Up	3.329	Up	0.0056	0.673	1.257	0.965
7	55839	<i>CENPN</i>	Centromere protein N	1	0	Up	4.295	Up	<0.0001	0.879	1.105	0.992
8	79019	<i>CENPM</i>	Centromere protein M	1	0	Up	29.162	Up	<0.0001	0.696	1.490	1.093
9	55722	<i>CEP72</i>	Centrosomal protein 72	1	2	Up	3.187	Up	<0.0001	0.896	1.313	1.104
10	25769	<i>SLC24A2</i>	Solute carrier family 24 (sodium/potassium/calcium exchanger), member 2	1	1	Up	3.610	Up	<0.0001	0.884	6.311	3.597
11	6664	<i>SOX11</i>	SRY (sex determining region Y)-box 11	1	0	Up	5.056	Up	<0.0001	0.460	26.297	13.378

Table III. Sequences of the primers used in the present study.

Gene	Forward (5'-3')	Reverse (5'-3')
<i>GUSB</i>	CGTCCCACCTAGAATCTGCT	TTGCTCACAAAGGTCACAGG
<i>ITGA3</i>	TCAACCTGGATACCCGATTCC	GCTCTGTCTGCCGATGGAG
<i>WDR62</i>	GCCTTCTCACCCAATATGAAGC	GCCTTCTCACCCAATATGAAGC
<i>ECT2</i>	ACTACTGGGAGGACTAGCTTG	CACCTCTGTTTCAATCTGAGGCA
<i>DNAJB13</i>	ATGGGCCAGGATTATTACTCTGT	GCTCATTGACTTCAACGGGTG
<i>CDKN3</i>	TCCGGGGCAATACAGACCAT	GCAGCTAATTTGTCCCGAAACTC
<i>CSPG5</i>	GCTGACTTACCCATTTTCAGGG	AGGGTGGTTCTCTGAGGTTCC
<i>CENPN</i>	TGAACTGACAACAATCCTGAAGG	CTTGACGCTTTTCCTCACAC
<i>CENPM</i>	GCGGACTCGATGCTCAAAGA	TTCTGGAGACTGTATTTGCTGTG
<i>CEP72</i>	CTCTCGCGAACTCCTTGG	GTGGAGCCGAAACACTTCTG
<i>SLC24A2</i>	GTCTGGTAGCCATTAGCACTG	TGGGCGTGATCTGTACTATTCTC
<i>SOX11</i>	AGCAAGAAATGCGGCAAGC	ATCCAGAAACACGCACTTGAC

GUSB, glucuronidase β ; *ITGA3*, Integrin alpha 3; *WDR62*, WD repeat domain 62; *ECT2*, Ect2 oncogene; *DNAJB13*, DnaJ (Hsp40) related, subfamily B, member 13; *CDKN3*, Cyclin-dependent kinase inhibitor 3; *CSPG5*, Chondroitin sulfate proteoglycan 5; *CENPN*, Centromere protein N; *CENPM*, Centromere protein M; *CEP72*, Centrosomal protein 72; *SLC24A2*, Solute carrier family 24 (sodium/potassium/calcium exchanger), member 2; *SOX11*, SRY (sex determining region Y)-box 11.

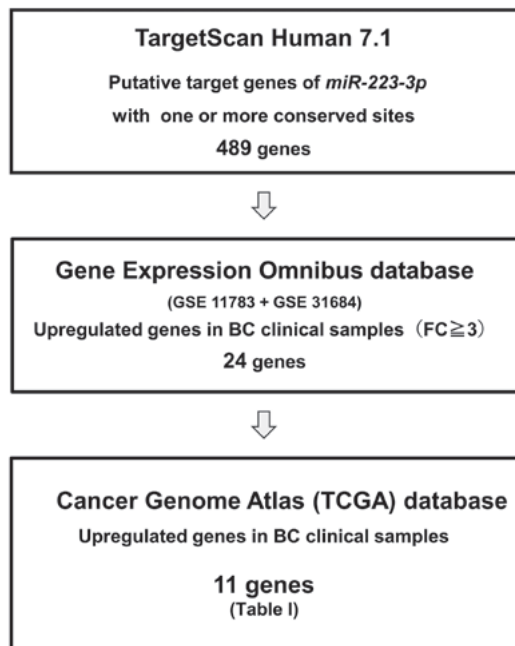


Figure 3. The strategy used to identify *miR-223* target genes. Flow chart for the *in silico* analysis of *miR-223* target genes. The 489 candidate target genes were identified by the TargetScan database. The analysis of gene expression was performed using available GEO datasets (GSE11783 and GSE31684) and the TCGA cohort database. The analyses revealed that 11 genes were significantly upregulated in BC. BC, bladder cancer.

expression level of *WDR62* was significantly higher in the non-papillary BC ($P<0.0001$), high-grade tumors ($P<0.0001$) and high-stage tumors ($P<0.01$; Fig. 5B). The higher expression level exhibited a trend towards significance in patients with BC with distant metastasis compared with their counterparts ($P=0.0528$; Fig. 5B). Subsequently, the cohort was divided into 2 groups according to the median *WDR62* expression level.

Kaplan-Meier analysis revealed no difference in the overall survival rate between patients with a high ($n=201$) and those with a low *WDR62* expression ($n=202$) ($P=0.5194$) (data not shown). In the BC samples ($n=32$) and normal bladder samples ($n=12$) from our facility, *WDR62* mRNA expression was significantly higher in the BC samples than in the normal bladder samples ($P<0.0095$; Fig. 6A). However, there was no significant association between *WDR62* expression and the patient clinicopathological parameters, such as non-papillary BC, high-grade tumors and high-stage tumors in clinical specimens from our facility (data not shown). Our cohort was too small to evaluate the precise statistical value.

IHC analysis of *WDR62* in a tissue microarray. We examined the expression level of *WDR62* in BC specimens by IHC staining. *WDR62* was strongly expressed in several tumor lesions (Fig. 6B, left panel), whereas a low expression was observed in the normal tissue (Fig. 6B, middle panel). Tissue microarray analysis revealed that the IHC score of the tumor tissues was significantly higher than that of the normal tissues ($P<0.0001$; Fig. 6B, right panel).

Effects of *WDR62* knockdown on the viability, migration and invasion of BC cell lines. To investigate the functional role of *WDR62* in BC cells, we performed loss-of-function experiments in the T24 and BOY cell lines transfected with 2 siRNA constructs targeting *WDR62* (*si-WDR62_1* and *si-WDR62_2*). The results of RT-qPCR and western blot analyses revealed that both siRNAs effectively decreased *WDR62* expression in both cell lines (Fig. S1). XTT assays then revealed a significant inhibition of viability in the *si-WDR62* transfectants compared with the mock or siRNA-control transfectants (each $P<0.0001$; Fig. 7A). In addition, colony formation assay confirmed that there was a significantly lower number of surviving BC cell colonies among the *si-WDR62* transfectants than among the mock or

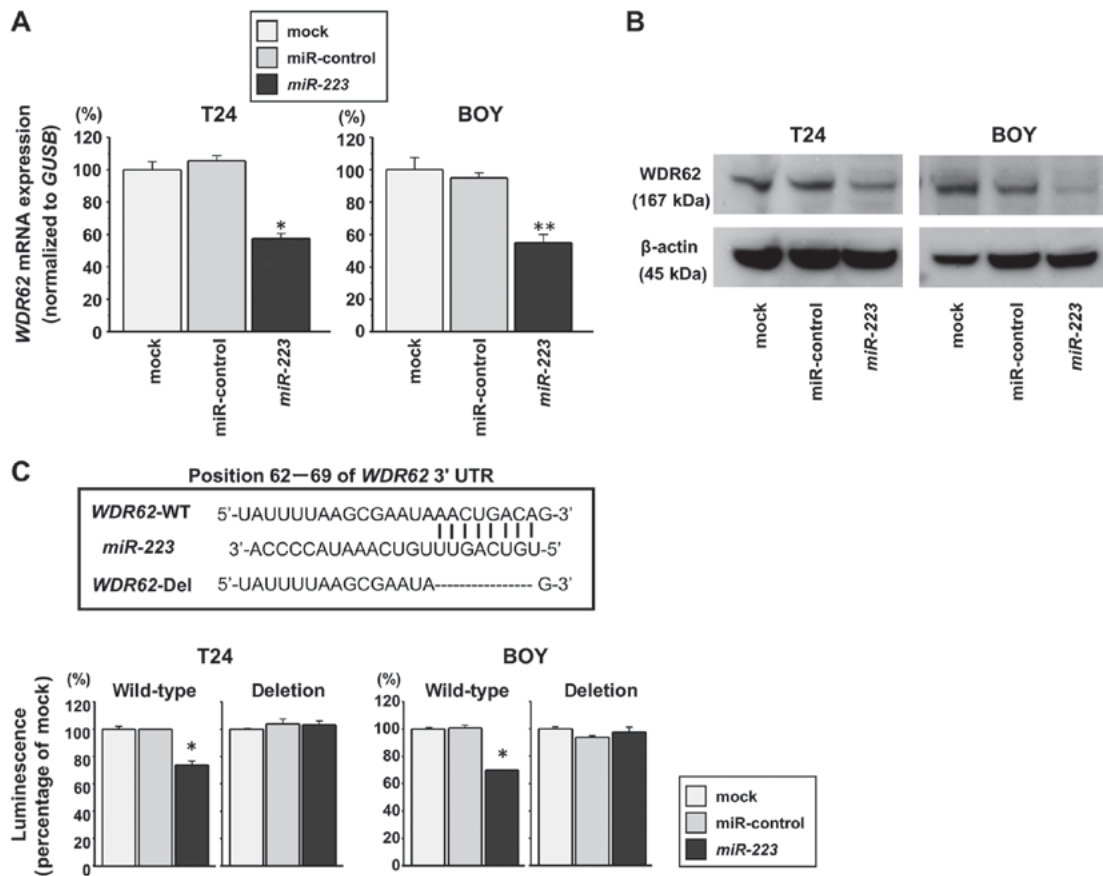


Figure 4. Direct regulation of WDR62 by *miR-223*. (A) WDR62 mRNA expression was evaluated by RT-qPCR in BC cells at 72 h following the transfection of *miR-223*. *GUSB* was used as an internal control. * $P=0.0002$ and ** $P=0.0012$. (B) WDR62 protein expression was evaluated by western blot analyses in BC cells at 72–96 h following the transfection of *miR-223*. β -actin was used as a loading control. (C) The *miR-223* binding site at position 62–69 within the 3'-UTR of WDR62 mRNA. Dual-luciferase reporter assays using vectors encoding the 3'-UTR containing this putative miRNA target site or that in which this site had been deleted. Normalized data are presented as *Renilla*/Firefly luciferase activity ratios. The luminescence intensity was significantly reduced by co-transfection with *miR-223* and the vector carrying the *miR-223* binding site. * $P<0.0001$. WDR62, WD repeat domain 62; BC, bladder cancer.

siRNA-control transfectants (each $P<0.0001$; Fig. 8). Wound healing assays also demonstrated that the cell migratory activity was significantly suppressed in the *si-WDR62* transfectants compared with the mock or siRNA-control transfectants (T24 cells: each $P<0.0001$; BOY cells: $P=0.0005$ and $P<0.0001$, respectively; Fig. 7B). Matrigel invasion assays demonstrated a significantly decreased number of invading cells among the *si-WDR62* transfectants compared with the mock or siRNA-control transfectants (T24 cells: each $P<0.0001$; BOY cells: $P=0.0277$ and $P<0.0001$, respectively; Fig. 7C).

Effects of WDR62 knockdown on the apoptosis of BC cell lines. We performed flow cytometric analyses to determine the number of apoptotic cells following the siRNA-mediated knockdown of WDR62 expression. There was a significantly greater number of apoptotic cells among the *si-WDR62* transfectants than among the mock or siRNA-control transfectants (T24 cells: each $P<0.0001$; BOY cells: $P<0.0001$ and $P=0.0147$, respectively; Fig. 7D). In addition, a caspase-3/7 activity assay revealed that the fluorescence intensity was significantly increased in the *si-WDR62* transfectants than in mock or siRNA-control transfectants (T24 cells: $P=0.0095$ and $P=0.0017$; BOY cells: $P=0.0045$ and $P=0.0001$, respectively; Fig. 7E). Moreover, the results of western blot analysis confirmed that cleaved caspase-3

and cleaved PARP expression increased in the *si-WDR62* transfectants in comparison with the mock or siRNA-control transfectants (Fig. 9).

Effects of *miR-223* restoration or WDR62 knockdown on the cell cycle of BC cell lines. To investigate the cell cycle effects, we performed flow cytometric analyses using *miR-223* or *si-WDR62* transfectants. Cell cycle assays revealed no fixed tendency in either transfectant (data not shown).

Effects of *miR-223* inhibition by anti-*miR-223* in BC cell lines. To confirm the roles of *miR-223*, we performed functional analyses using BC cells co-transfected with *miR-223* and *anti-miR-223*. The results of RT-qPCR and western blot analyses revealed that co-transfection with *anti-miR-223* and *miR-223* recovered the WDR62 mRNA and protein expression levels that were suppressed by transfection *miR-223* with alone (Fig. 10A and B, respectively). XTT assays revealed that cell viability was restored in the cells co-transfected with *anti-miR-223* and *miR-223* in comparison with that of the cells transfected with *miR-223* alone (each $P<0.0001$; Fig. 10C). Wound healing and Matrigel invasion assays also demonstrated that the migratory and invasive activity was significantly restored in the cells co-transfected with *anti-miR-223* and *miR-223* in comparison with the cells transfected with

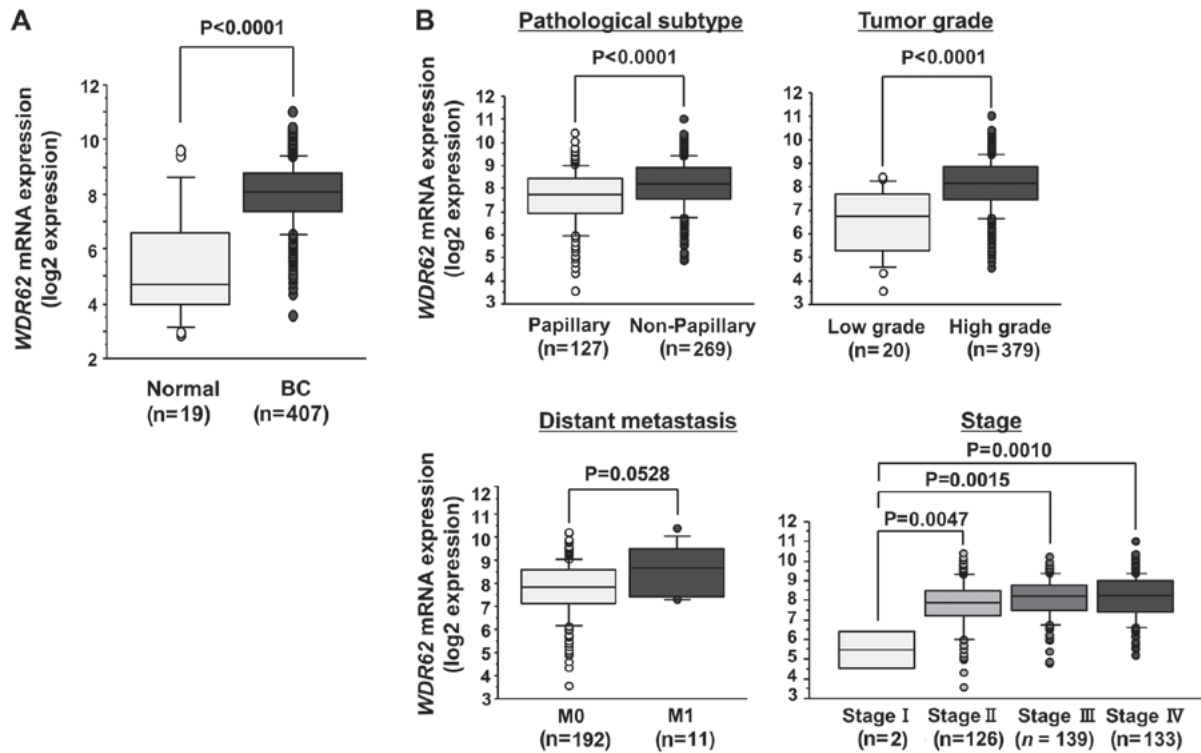


Figure 5. Associations of the expression level of *WDR62* with patient clinicopathological parameters. (A) Among the BC cohort of TCGA, the mRNA expression level of *WDR62* was significantly higher in BC samples compared with normal bladder samples. (B) The associations between *WDR62* expression and clinicopathological parameters of the cohort of TCGA were determined using the Mann-Whitney U test. *WDR62*, *WD repeat domain 62*; BC, bladder cancer.

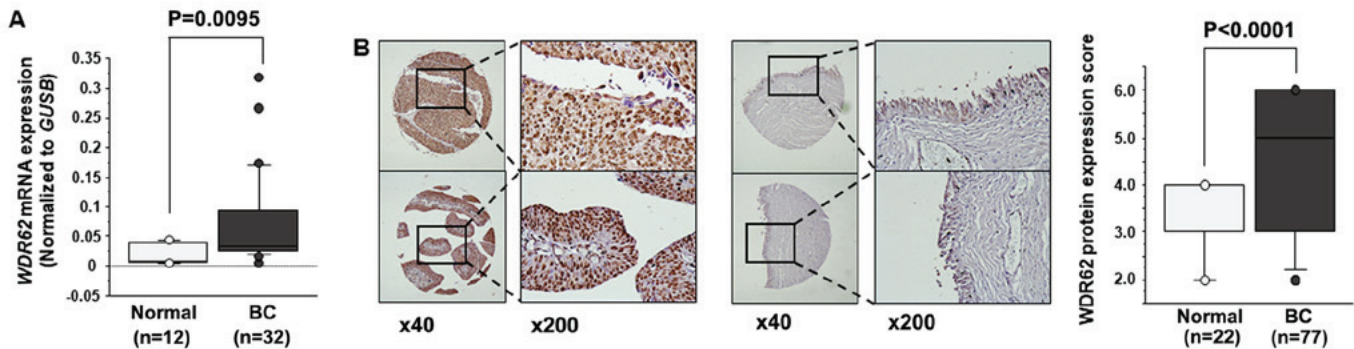


Figure 6. *WDR62* expression in clinical BC specimens. (A) The mRNA expression level of *WDR62*, determined by RT-qPCR, was significantly higher in the 32 clinical BC specimens than in the 12 adjacent NBE specimens from our facility. (B) Representative immunohistochemical staining of *WDR62* in BC specimens (left panel) and normal tissues (middle panel). The protein expression score was significantly higher in 77 clinical BC specimens than in 22 normal tissues from the tissue microarray analysis (right panel). *WDR62*, *WD repeat domain 62*; BC, bladder cancer.

miR-223 alone (each $P<0.0001$; Fig. 10D and E, respectively). These findings suggest that *miR-223* suppresses cell viability, migration and invasion through *WDR62* knockdown in BC.

Discussion

The aberrant expression of miRNAs has been found in a number of types of human cancer and plays significant roles in oncogenesis and metastasis (9). Therefore, the detection of aberrantly expressed miRNAs and their target genes is important for the elucidation of miRNA-regulated oncogenic pathways. Many genome-wide miRNA expression analyses, including deep sequencing, have been applied for the evaluation of several types of cancer. In our previous studies,

the *miR-1/133a* cluster, *miR-23b/27b* cluster, *miR-135a*, *miR-138*, *miR-143/145* cluster, *miR-200* family (*miR-200a/b/c*, *miR-141* and *miR-429*), *miR-218*, *miR-1285* and *miR-1291* were found to be frequently decreased in renal cell carcinoma, and these miRNAs have been identified as tumor suppressors by targeting several oncogenic genes (20-28).

Our previous deep sequencing analysis in BC revealed that *miR-223* expression was decreased in BC tissues compared with normal bladder tissues (10). Zhi *et al* and Guo *et al* demonstrated that *miR-223* inhibited the migration and invasion of BC cell lines (29,30). These findings suggest that *miR-223* may function as a tumor suppressor in BC. However, the analysis of the functional role of *miR-223* has yielded controversial results in previous studies. In studies on gastric cancer, colorectal cancer

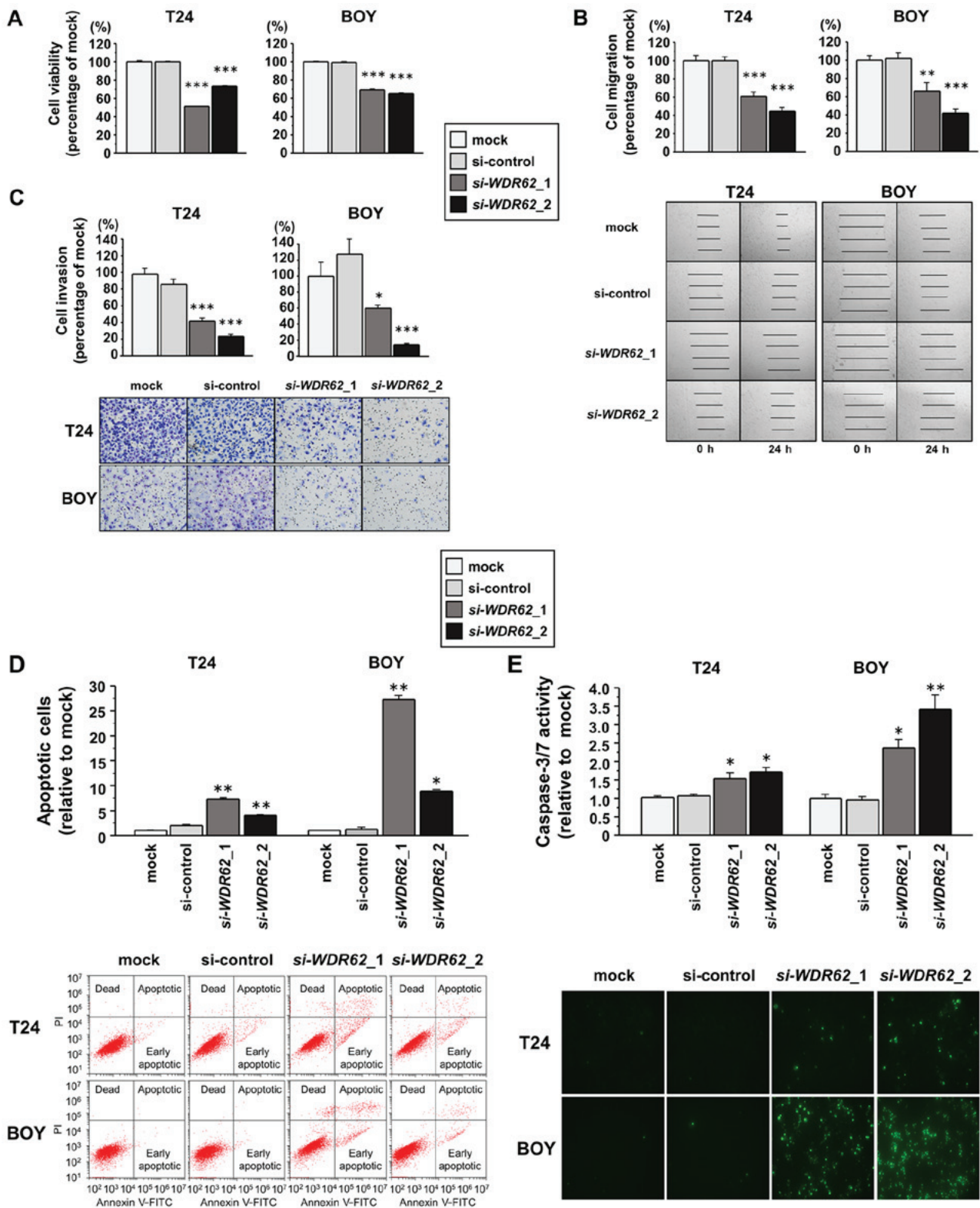


Figure 7. Effects of *WDR62* knockdown on BC cell lines. (A-C) Cell viability, migration and invasion were determined by (A) XTT, (B) wound healing and (C) Matrigel invasion assays, respectively. * $P=0.0277$, ** $P=0.0005$ and *** $P<0.0001$. (D) The numbers of apoptotic cells were measured by flow cytometry. Normalized apoptotic cell ratios are presented in the histograms. * $P=0.0147$ and ** $P<0.0001$. (E) Caspase-3/7 activity was measured by a fluorescence-based assay. The normalized fluorescence intensity ratios are shown in the histograms. * $P<0.01$ and ** $P=0.0001$. *WDR62*, *WD repeat domain 62*; BC, bladder cancer.

and vulvar carcinoma (31-34), *miR-223* has been reported to be an oncogenic miRNA. On the other hand, *miR-223* has been reported to function as a tumor suppressor miRNA in prostate cancer, breast cancer, cervical cancer and acute myeloid leukemia (19,35-37). In support of its tumor-suppressive

role, Kurozumi *et al* demonstrated that *miR-223* inhibited the migration and invasion of prostatic cancer cells (37), and Xiao *et al* demonstrated that *miR-223* inhibited the proliferation and enhanced the apoptosis of acute myeloid leukemia cell lines (19). The present study revealed that restoration of *miR-223*

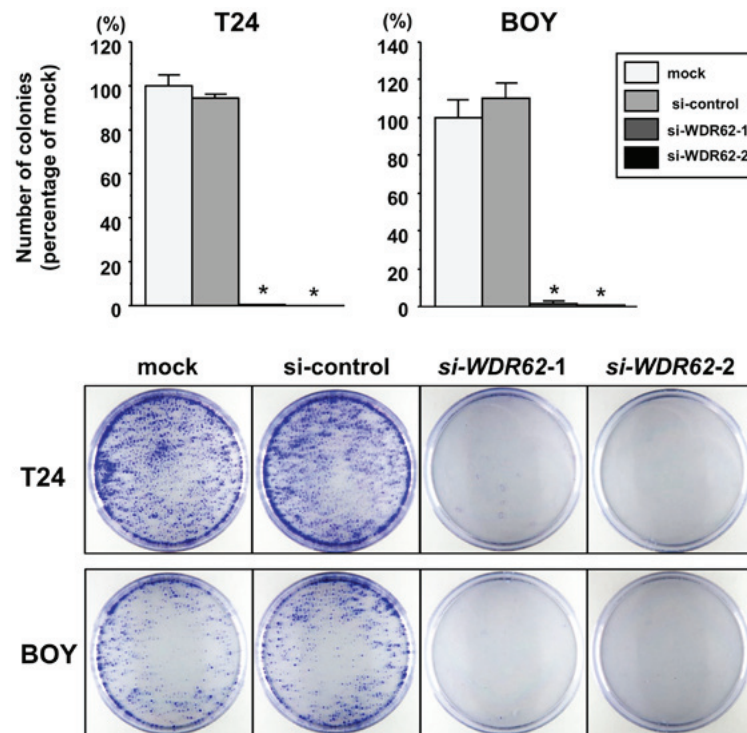


Figure 8. Effects of *WDR62* knockdown on BC cell lines in colony formation assays. There were significantly less number of surviving BC cell colonies among the *si-WDR62* transfectants than among the mock or siRNA-control respectively transfectants (upper panels) and the representative colony formation images (lower panels). *WDR62*, *WD repeat domain 62*; BC, bladder cancer. * $P < 0.0001$.

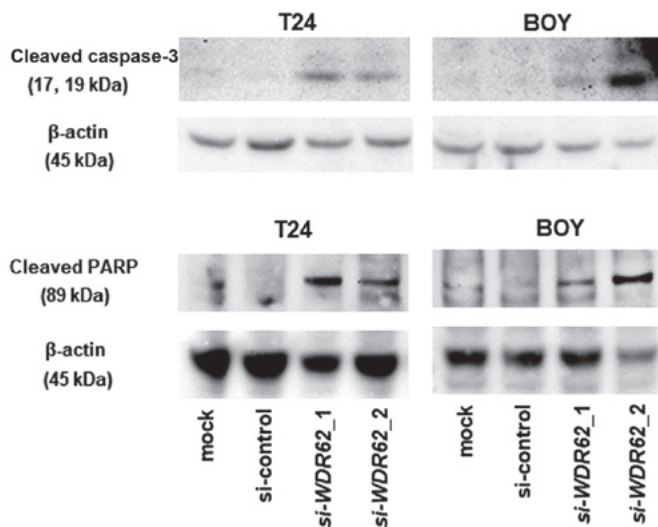


Figure 9. Effects of *WDR62* knockdown on BC cell lines examined by western blot analyses for apoptotic markers. Cleaved form of both caspase-3 and PARP expression were evaluated by western blot analyses in the *si-WDR62* transfectants than among the mock or siRNA-control transfectants in BC cells. β -actin was used as a loading control. *WDR62*, *WD repeat domain 62*; BC, bladder cancer; PARP, poly(ADP-ribose) polymerase.

markedly suppressed the viability, migration and invasion, and induced the apoptosis of BC cells, suggesting that *miR-223* may function as a tumor suppressor miRNA in BC.

According to our *miR-223* target analyses, we focused on the *WDR62* gene. *WDR62* is a recently identified centrosome-associated protein that plays important roles in DNA replication and cell cycle progression (38). *WDR62* was originally reported as a scaffold protein associated with the

JNK pathway. *WDR62* consists of 13 repeats of the WD40 domain in its N-terminal half and MKK7/JNK binding domains and 6 potential JNK phosphorylation sites in its C-terminal half, and it mediates cell signaling, transcriptional, mitotic and apoptotic functions (39-41). Of note, *WDR62* expression was observed in the spindle poles of dividing cells, but not in the nucleus during mitosis, suggesting a critical role of *WDR62* in cell proliferation (42). Previous studies have revealed that *WDR62* plays important roles in cerebral cortical development, and mutations in its gene have been associated with microcephaly (42-45). However, to the best of our knowledge, the functional roles of *WDR62* in human cancer remain unclear, as there are only 3 reports available regarding the functional roles of *WDR62* in human cancer (38,46-47). Zeng *et al* demonstrated that suppression of *WDR62* induced G2/M cell cycle arrest and apoptosis, and its expression was associated with chemoresistance and a poor prognosis in gastric cancer (46). Zhang *et al* demonstrated that *WDR62* overexpression may be related to centrosome amplification in ovarian cancer (47). Shinmura *et al* demonstrated that *WDR62* overexpression was associated with a poor prognosis and centrosome amplification in lung adenocarcinoma (38). In nerve cells, the upregulation of *WDR62* has been shown to induce cell apoptosis via the JNK pathway (41). Conversely, in this study, the downregulation of *WDR62* induced the apoptosis and inhibited the viability of BC cells. The functional roles of *WDR62* may differ between benign and cancer tissues. Therefore, there seems to be no association between *WDR62* with the JNK pathway in BC. Further studies are warranted to identify other pathways related to *WDR62* in BC.

In addition, we found that *WDR62* knockdown suppressed cell invasion and migration, which has not been reported

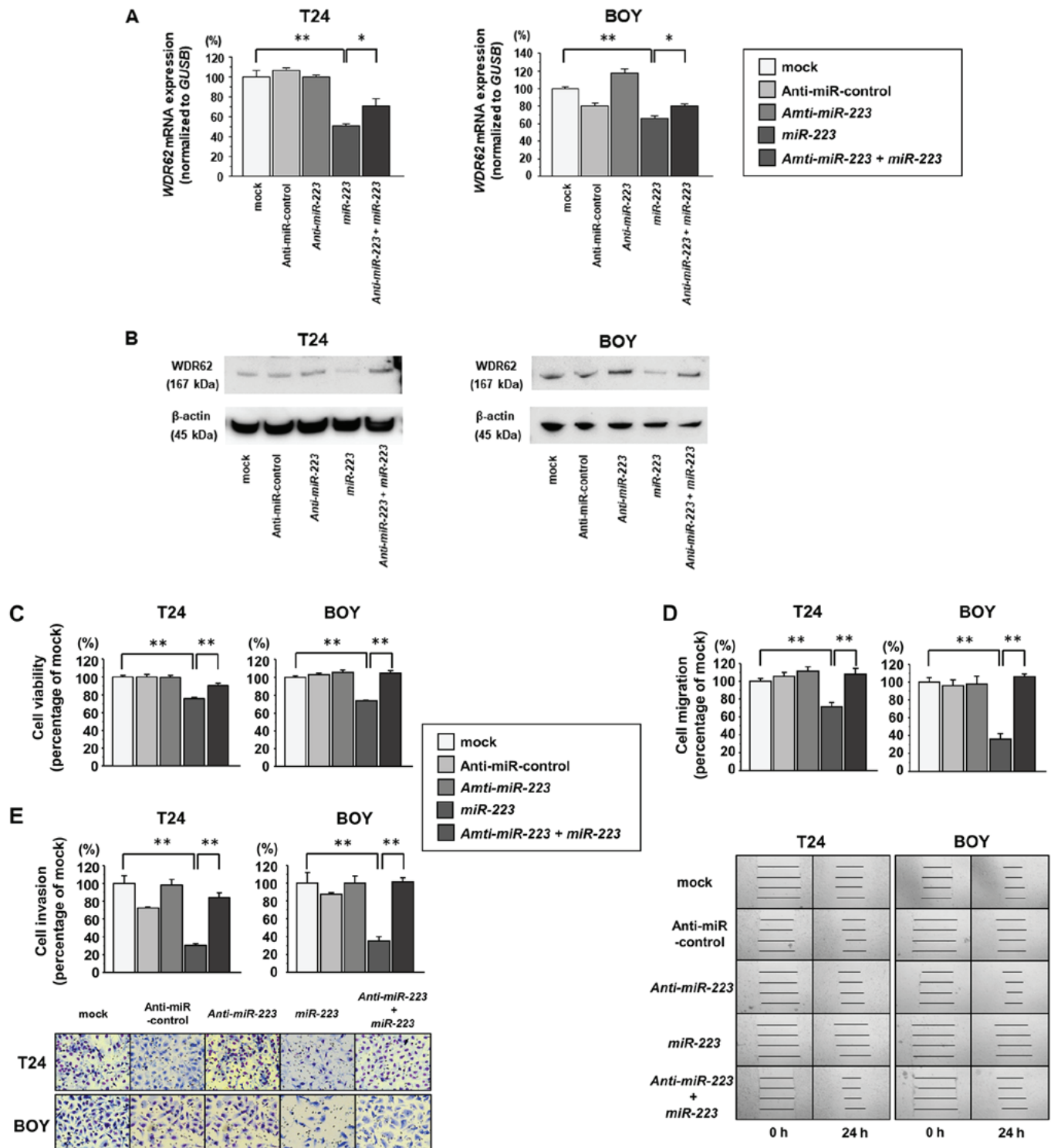


Figure 10. Effects of the inhibition of miR-223 in BC cell lines. (A and B) WDR62 expression levels were evaluated in BC cells at 72 h following the co-transfection of *anti-miR-223* and *miR-223* into BC cells by (A) RT-qPCR and (B) western blot analyses. GUSB and β -actin was used as a control. *Anti-miR-223* recovered WDR62 mRNA and protein expression levels, which were suppressed by transfection with *miR-223* alone. * $P < 0.05$ and ** $P < 0.0001$. (C-E) Cell viability, migration and invasion were determined by (C) XTT, (D) wound healing and (E) Matrigel invasion assays, respectively. *Anti-miR-223* recovered cell viability, migration and invasion, which was suppressed by transfection with *miR-223* alone. ** $P < 0.0001$.

previously. Notably, two of the three previous reports indicated that *WDR62* overexpression was associated with centrosome amplification in distinct types of cancer. Centrosome amplification is an abnormal cellular process in which cells acquire three or more centrosomes, and it results in multipolar mitosis, the consequences of which may include mitotic

catastrophe or delayed mitotic progression (48,49). In addition, aberrant mitoses may result in the acquisition of aneuploidy and chromosome instability (50,51). Centrosome amplification is well known as a common feature of many types of cancer; however, its effect on cancer is not yet fully understood. Raff *et al* demonstrated that centrosome amplification initiated

tumorigenesis in a mouse model (52). Godinho *et al* suggested that centrosome amplification was involved in cellular invasions (53). Centrosome amplification may be an important mechanism of the oncogenic role of *WDR62*. Further studies are warranted to clarify this hypothesis.

In this study, the analyses of the TCGA database indicated that *WDR62* expression, as well as *miR-223* expression, may be associated with distant metastasis. Moreover, *WDR62* knockdown, as well as *miR-223* restoration, inhibited the migration and invasion of BC cells. However, the analyses of the TCGA database revealed that *miR-223* or *WDR62* expression was not related to the survival rate. The upregulation of oncogenic *WDR62* due to the suppression of *miR-223* may be an important mechanism for cell invasion and metastasis in BC cells. However, it is not a critical factor that affects disease survival in BC. In addition, no significant inverse correlation was detected between *miR-223* and *WDR62* mRNA expression in the TCGA database (data not shown). A number of miRNAs, including *miR-223* target *WDR62*, implying that *miR-223* alone does not suppress *WDR62* expression with statistical significance. Further studies are warranted to elucidate other regulatory factors of *WDR62* expression.

In conclusion, in this study, *miR-223* was shown to function as a tumor suppressor in BC cells. To the best of our knowledge, this is the first report demonstrating that the tumor suppressor *miR-223* directly regulates *WDR62* in BC cells. The identification of novel molecular pathways and targets regulated by the *miR-223/WDR62* axis may provide important insight into the potential mechanisms of BC progression.

Acknowledgements

The authors would like to thank Ms. Mutsumi Miyazaki for her excellent laboratory assistance.

Funding

This study was supported by the KAKENHI (KIBAN-B) 16H05464 and 17H04332, KAKENHI (KIBAN-C) 16K11015, KAKENHI (WAKATE-B) 17K16799.

Availability of data and materials

All data generated or analyzed during this study are included in this published article or are available from the corresponding author on reasonable request.

Authors' contributions

SS, HY, MY, HE and MN conceived of the study and designed the experiments. SS, HY, KM, RM and TS performed the experiments. TI and ST contributed to the interpretation of the data. SS, TI, ST and HE drafted the manuscript. All authors have reviewed the manuscript and approved the final version.

Ethics approval and consent to participate

This study was approved by the Bioethics Committee of Kagoshima University; the study approval numbers were

H27-104 and H27-105. Written informed consent and approval were obtained from all patients prior to obtaining the samples.

Patient consent for publication

Not applicable.

Competing interests

The authors declare that they have no competing interests.

References

1. Ferlay J, Steliarova-Foucher E, Lortet-Tieulent J, Rosso S, Coebergh JW, Comber H, Forman D and Bray F: Cancer incidence and mortality patterns in Europe: Estimates for 40 countries in 2012. *Eur J Cancer* 49: 1374-1403, 2013.
2. Torre LA, Bray F, Siegel RL, Ferlay J, Lortet-Tieulent J and Jemal A: Global cancer statistics, 2012. *CA Cancer J Clin* 65: 87-108, 2015.
3. Vale C; Advanced Bladder Cancer Meta-analysis Collaboration: Neoadjuvant chemotherapy in invasive bladder cancer: A systematic review and meta-analysis. *Lancet* 361: 1927-1934, 2003.
4. von der Maase H, Hansen SW, Roberts JT, Dogliotti L, Oliver T, Moore MJ, Bodrogi I, Albers P, Knuth A, Lippert CM, *et al*: Gemcitabine and cisplatin versus methotrexate, vinblastine, doxorubicin, and cisplatin in advanced or metastatic bladder cancer: Results of a large, randomized, multinational, multicenter, phase III study. *J Clin Oncol* 18: 3068-3077, 2000.
5. Meeks JJ, Bellmunt J, Bochner BH, Clarke NW, Daneshmand S, Galsky MD, Hahn NM, Lerner SP, Mason M, Powles T, *et al*: A systematic review of neoadjuvant and adjuvant chemotherapy for muscle-invasive bladder cancer. *Eur Urol* 62: 523-533, 2012.
6. Carthew RW and Sontheimer EJ: Origins and Mechanisms of miRNAs and siRNAs. *Cell* 136: 642-655, 2009.
7. Friedman RC, Farh KK, Burge CB and Bartel DP: Most mammalian mRNAs are conserved targets of microRNAs. *Genome Res* 19: 92-105, 2009.
8. Lewis BP, Shih IH, Jones-Rhoades MW, Bartel DP and Burge CB: Prediction of mammalian microRNA targets. *Cell* 115: 787-798, 2003.
9. Calin GA and Croce CM: MicroRNA signatures in human cancers. *Nat Rev Cancer* 6: 857-866, 2006.
10. Itesako T, Seki N, Yoshino H, Chiyomaru T, Yamasaki T, Hidaka H, Yonezawa T, Nohata N, Kinoshita T, Nakagawa M, *et al*: The microRNA expression signature of bladder cancer by deep sequencing: The functional significance of the miR-195/497 cluster. *PLoS One* 9: e84311, 2014.
11. Ichimi T, Enokida H, Okuno Y, Kunimoto R, Chiyomaru T, Kawamoto K, Kawahara K, Toki K, Kawakami K, Nishiyama K, *et al*: Identification of novel microRNA targets based on microRNA signatures in bladder cancer. *Int J Cancer* 125: 345-352, 2009.
12. Livak KJ and Schmittgen TD: Analysis of relative gene expression data using real-time quantitative PCR and the 2(-ΔΔC(T)) method. *Methods* 25: 402-408, 2001.
13. Yoshino H, Chiyomaru T, Enokida H, Kawakami K, Tatarano S, Nishiyama K, Nohata N, Seki N and Nakagawa M: The tumour-suppressive function of miR-1 and miR-133a targeting TAGLN2 in bladder cancer. *Br J Cancer* 104: 808-818, 2011.
14. Matsushita R, Seki N, Chiyomaru T, Inoguchi S, Ishihara T, Goto Y, Nishikawa R, Mataka H, Tatarano S, Itesako T, *et al*: Tumour-suppressive microRNA-144-5p directly targets CCNE1/2 as potential prognostic markers in bladder cancer. *Br J Cancer* 113: 282-289, 2015.
15. Block AL, Bauer KD, Williams TJ and Seidenfeld J: Experimental parameters and a biological standard for acridine orange detection of drug-induced alterations in chromatin condensation. *Cytometry* 8: 163-169, 1987.
16. Kumar A, Sahu SK, Mohanty S, Chakrabarti S, Maji S, Reddy RR, Jha AK, Goswami C, Kundu CN, Rajasubramaniam S, *et al*: Kaposi sarcoma herpes virus latency associated nuclear antigen protein release the G2/M cell cycle blocks by modulating ATM/ATR mediated checkpoint pathway. *PLoS One* 9: e100228, 2014.

17. Bradford MM: A rapid and sensitive method for the quantitation of microgram quantities of protein utilizing the principle of protein-dye binding. *Anal Biochem* 72: 248-254, 1976.
18. Li B and Dewey CN: RSEM: Accurate transcript quantification from RNA-Seq data with or without a reference genome. *BMC Bioinformatics* 12: 323, 2011.
19. Xiao Y, Su C and Deng T: miR-223 decreases cell proliferation and enhances cell apoptosis in acute myeloid leukemia via targeting FBXW7. *Oncol Lett* 12: 3531-3536, 2016.
20. Kawakami K, Enokida H, Chiyomaru T, Tatarano S, Yoshino H, Kagara I, Gotanda T, Tachiwada T, Nishiyama K, Nohata N, *et al*: The functional significance of miR-1 and miR-133a in renal cell carcinoma. *Eur J Cancer* 48: 827-836, 2012.
21. Ishihara T, Seki N, Inoguchi S, Yoshino H, Tatarano S, Yamada Y, Itesako T, Goto Y, Nishikawa R, Nakagawa M, *et al*: Expression of the tumor suppressive miRNA-23b/27b cluster is a good prognostic marker in clear cell renal cell carcinoma. *J Urol* 192: 1822-1830, 2014.
22. Yamada Y, Hidaka H, Seki N, Yoshino H, Yamasaki T, Itesako T, Nakagawa M and Enokida H: Tumor-suppressive microRNA-135a inhibits cancer cell proliferation by targeting the c-MYC oncogene in renal cell carcinoma. *Cancer Sci* 104: 304-312, 2013.
23. Yamasaki T, Seki N, Yamada Y, Yoshino H, Hidaka H, Chiyomaru T, Nohata N, Kinoshita T, Nakagawa M and Enokida H: Tumor suppressive microRNA 138 contributes to cell migration and invasion through its targeting of vimentin in renal cell carcinoma. *Int J Oncol* 41: 805-817, 2012.
24. Yoshino H, Enokida H, Itesako T, Kojima S, Kinoshita T, Tatarano S, Chiyomaru T, Nakagawa M and Seki N: Tumor-suppressive microRNA-143/145 cluster targets hexokinase-2 in renal cell carcinoma. *Cancer Sci* 104: 1567-1574, 2013.
25. Yoshino H, Enokida H, Itesako T, Tatarano S, Kinoshita T, Fuse M, Kojima S, Nakagawa M and Seki N: Epithelial-mesenchymal transition-related microRNA-200s regulate molecular targets and pathways in renal cell carcinoma. *J Hum Genet* 58: 508-516, 2013.
26. Yamasaki T, Seki N, Yoshino H, Itesako T, Hidaka H, Yamada Y, Tatarano S, Yonezawa T, Kinoshita T, Nakagawa M, *et al*: MicroRNA-218 inhibits cell migration and invasion in renal cell carcinoma through targeting caveolin-2 involved in focal adhesion pathway. *J Urol* 190: 1059-1068, 2013.
27. Hidaka H, Seki N, Yoshino H, Yamasaki T, Yamada Y, Nohata N, Fuse M, Nakagawa M and Enokida H: Tumor suppressive microRNA-1285 regulates novel molecular targets: Aberrant expression and functional significance in renal cell carcinoma. *Oncotarget* 3: 44-57, 2012.
28. Yamasaki T, Seki N, Yoshino H, Itesako T, Yamada Y, Tatarano S, Hidaka H, Yonezawa T, Nakagawa M and Enokida H: Tumor-suppressive microRNA-1291 directly regulates glucose transporter 1 in renal cell carcinoma. *Cancer Sci* 104: 1411-1419, 2013.
29. Zhi Y, Pan J, Shen W, He P, Zheng J, Zhou X, Lu G, Chen Z and Zhou Z: Ginkgolide B inhibits human bladder cancer cell migration and invasion through microRNA-223-3p. *Cell Physiol Biochem* 39: 1787-1794, 2016.
30. Guo J, Cao R, Yu X, Xiao Z and Chen Z: MicroRNA-223-3p inhibits human bladder cancer cell migration and invasion. *Tumour Biol* 39: 1010428317691678, 2017.
31. Zhou X, Jin W, Jia H, Yan J and Zhang G: MiR-223 promotes the cisplatin resistance of human gastric cancer cells via regulating cell cycle by targeting FBXW7. *J Exp Clin Cancer Res* 34: 28, 2015.
32. Eto K, Iwatsuki M, Watanabe M, Ishimoto T, Ida S, Imamura Y, Iwagami S, Baba Y, Sakamoto Y, Miyamoto Y, *et al*: The sensitivity of gastric cancer to trastuzumab is regulated by the miR-223/FBXW7 pathway. *Int J Cancer* 136: 1537-1545, 2015.
33. Li ZW, Yang YM, Du LT, Dong Z, Wang LL, Zhang X, Zhou XJ, Zheng GX, Qu AL and Wang CX: Overexpression of miR-223 correlates with tumor metastasis and poor prognosis in patients with colorectal cancer. *Med Oncol* 31: 256, 2014.
34. de Melo Maia B, Rodrigues IS, Akagi EM, Soares do Amaral N, Ling H, Monroig P, Soares FA, Calin GA and Rocha RM: MiR-223-5p works as an oncomiR in vulvar carcinoma by TP63 suppression. *Oncotarget* 7: 49217-49231, 2016.
35. Sun X, Li Y, Zheng M, Zuo W and Zheng W: MicroRNA-223 increases the sensitivity of triple-negative breast cancer stem cells to TRAIL-induced apoptosis by targeting HAX-1. *PLoS One* 11: e0162754, 2016.
36. Tang Y, Wang Y, Chen Q, Qiu N, Zhao Y and You X: MiR-223 inhibited cell metastasis of human cervical cancer by modulating epithelial-mesenchymal transition. *Int J Clin Exp Pathol* 8: 11224-11229, 2015.
37. Kurozumi A, Goto Y, Matsushita R, Fukumoto I, Kato M, Nishikawa R, Sakamoto S, Enokida H, Nakagawa M, Ichikawa T, *et al*: Tumor-suppressive microRNA-223 inhibits cancer cell migration and invasion by targeting ITGA3/ITGB1 signaling in prostate cancer. *Cancer Sci* 107: 84-94, 2016.
38. Shinmura K, Kato H, Kawanishi Y, Igarashi H, Inoue Y, Yoshimura K, Nakamura S, Fujita H, Funai K, Tanahashi M, *et al*: WDR62 overexpression is associated with a poor prognosis in patients with lung adenocarcinoma. *Mol Carcinog* 56: 1984-1991, 2017.
39. Wasserman T, Katsenelson K, Daniluc S, Hasin T, Choder M and Aronheim A: A novel c-Jun N-terminal kinase (JNK)-binding protein WDR62 is recruited to stress granules and mediates a nonclassical JNK activation. *Mol Biol Cell* 21: 117-130, 2010.
40. Cohen-Katsenelson K, Wasserman T, Khateb S, Whitmarsh AJ and Aronheim A: Docking interactions of the JNK scaffold protein WDR62. *Biochem J* 439: 381-390, 2011.
41. Kuan CY, Yang DD, Samanta Roy DR, Davis RJ, Rakic P and Flavell RA: The Jnk1 and Jnk2 protein kinases are required for regional specific apoptosis during early brain development. *Neuron* 22: 667-676, 1999.
42. Nicholas AK, Khurshid M, Désir J, Carvalho OP, Cox JJ, Thornton G, Kausar R, Ansar M, Ahmad W, Verloes A, *et al*: WDR62 is associated with the spindle pole and is mutated in human microcephaly. *Nat Genet* 42: 1010-1014, 2010.
43. Yu TW, Mochida GH, Tischfield DJ, Sgaier SK, Flores-Sarnat L, Sergi CM, Topcu M, McDonald MT, Barry BJ, Felie JM, *et al*: Mutations in WDR62, encoding a centrosome-associated protein, cause microcephaly with simplified gyri and abnormal cortical architecture. *Nat Genet* 42: 1015-1020, 2010.
44. Xu D, Zhang F, Wang Y, Sun Y and Xu Z: Microcephaly-associated protein WDR62 regulates neurogenesis through JNK1 in the developing neocortex. *Cell Rep* 6: 104-116, 2014.
45. Pervaiz N and Abbasi AA: Molecular evolution of WDR62, a gene that regulates neocorticalogenesis. *Meta Gene* 9: 1-9, 2016.
46. Zeng S, Tao Y, Huang J, Zhang S, Shen L, Yang H, Pei H, Zhong M, Zhang G, Liu T, *et al*: WD40 repeat-containing 62 overexpression as a novel indicator of poor prognosis for human gastric cancer. *Eur J Cancer* 49: 3752-3762, 2013.
47. Zhang Y, Tian Y, Yu JJ, He J, Luo J, Zhang S, Tang CE and Tao YM: Overexpression of WDR62 is associated with centrosome amplification in human ovarian cancer. *J Ovarian Res* 6: 55, 2013.
48. Fukasawa K: Oncogenes and tumour suppressors take on centrosomes. *Nat Rev Cancer* 7: 911-924, 2007.
49. Godinho SA, Kwon M and Pellman D: Centrosomes and cancer: How cancer cells divide with too many centrosomes. *Cancer Metastasis Rev* 28: 85-98, 2009.
50. Anderhub SJ, Krämer A and Maier B: Centrosome amplification in tumorigenesis. *Cancer Lett* 322: 8-17, 2012.
51. Chan JY: A clinical overview of centrosome amplification in human cancers. *Int J Biol Sci* 7: 1122-1144, 2011.
52. Raff JW and Basto R: Centrosome Amplification and Cancer: A Question of Sufficiency. *Dev Cell* 40: 217-218, 2017.
53. Godinho SA, Picone R, Burute M, Dagher R, Su Y, Leung CT, Polyak K, Brugge JS, Théry M and Pellman D: Oncogene-like induction of cellular invasion from centrosome amplification. *Nature* 510: 167-171, 2014.